Journal of Chromatography A, 1218 (2011) 3862–3875

Contents lists available at ScienceDirect

Journal of Chromatography A

journal homepage: www.elsevier.com/locate/chroma

Efficient organic monoliths prepared by γ-radiation induced polymerization in the evaluation of histone deacetylase inhibitors by capillary(nano)-high performance liquid chromatography and ion trap mass spectrometry

Elena Badaloni[a], Marcella Barbarino[a], Walter Cabri[a,*], Ilaria D'Acquarica[b], Michela Forte[a], Francesco Gasparrini[b,*], Fabrizio Giorgi[a], Marco Pierini[b], Patrizia Simone[b], Ornella Ursini[c], Claudio Villani[b]

[a] sigma-tau S.p.A., R&D Department, Via Pontina km 30,400, 00040 Pomezia, Italy
[b] Dipartimento di Chimica e Tecnologie del Farmaco, Sapienza Università di Roma, P.le Aldo Moro 5, 00185 Roma, Italy
[c] Istituto di Metodologie Chimiche, Area della Ricerca di Roma del CNR, 00016 Monterotondo Stazione, Roma, Italy

ARTICLE INFO

Article history:
Received 18 February 2011
Received in revised form 14 April 2011
Accepted 16 April 2011
Available online 27 April 2011

Keywords:
Cap(nano)-LC
Polymethacrylate organic monoliths
γ-Radiation induced polymerization
Histone deacetylase (HDAC) inhibitors (HDACi)
Post-translational modifications (PTMs)
Suberoylanilide hydroxamic acid (SAHA)

ABSTRACT

New monolithic HPLC columns were prepared by γ-radiation-triggered polymerization of hexyl methacrylate and ethylene glycol dimethacrylate monomers in the presence of porogenic solvents. Polymerization was carried out directly within capillary (250–200 μm I.D.) and nano (100–75 μm I.D.) fused-silica tubes yielding highly efficient columns for cap(nano)-LC applications. The columns were applied in the complete separation of core (H2A, H2B, H3, and H4) and linker (H1) histones under gradient elution with UV and/or electrospray ionization (ESI) ion trap mass spectrometry (MS) detections. Large selectivity towards H1, H2A-1, H2A-2, H2B, H3-1, H3-2 and H4 histones and complete separation were obtained within 8 min time windows, using fast gradients and very high linear flow velocities, up to 11 mm/s for high throughput applications. The method developed was the basis of a simple and efficient protocol for the evaluation of post-translational modifications (PTMs) of histones from NCI-H460 human non-small-cell lung cancer (NSCLC) and HCT-116 human colorectal carcinoma cells. The study was extended to monitoring the level of histone acetylation after inhibition of Histone DeACetylase (HDAC) enzymes with suberoylanilide hydroxamic acid (SAHA), the first HDAC inhibitor approved by the FDA for cancer therapy. Attractive features of our cap(nano)-LC/MS approach are the short analysis time, the minute amount of sample required to complete the whole procedure and the stability of the polymethacrylate-based columns. A lab-made software package ClustMass was *ad hoc* developed and used to elaborate deconvoluted mass spectral data (aligning, averaging, clustering) and calculate the potency of HDAC inhibitors, expressed through a Relative half maximal Inhibitory Concentration parameter, namely R_IC$_{50}$ and an averaged acetylation degree.

1. Introduction

In the nucleus of all eukaryotic cells genomic DNA is highly folded, constrained, and compacted by proteins in a dynamic polymer known as chromatin [1]. The principal protein components of chromatin are small basic proteins called histones, including core histones (namely H2A, H2B, H3, and H4) and the linker histones H1 [2]. Although it was first assumed that the purpose of histones was to compress the DNA to fit within the nucleus, subsequent research suggested that histones are not merely packaging factors, but function to regulate gene expression [3,4]. Since then, the field of histone proteomics is largely expanding, due to increasing evidence of the diverse regulatory roles played by this group of proteins. In particular, post-translational modifications (PTMs) of specific residues in the *N*-terminal tails of core histones have been demonstrated to be critical to their regulatory function [5–7]. PTMs affect lysines (acetylation, mono-, di-, and trimethylation), serines and threonines (phosphorylation), and arginines (mono- and two types of dimethylation) [8–10]. Such modifications can alter the global dynamics of chromatin structure and function [11,12] and constitute the basis for the "histone code" hypothesis [1,13]. Traditional methods for the study of histone PTMs include micro-sequencing and immunoassay methods [14,15]. Micro-sequencing is tedious and requires relatively large amount of purified protein. Immunoassays are very sensitive, but rely on highly specific antibodies that recognize different modification sites. Mass spectrometry is likely to play a fundamental role in the characterization

* Corresponding authors. Tel.: +39 06 49912776; fax: +39 06 49912780.
E-mail addresses: walter.cabri@sigma-tau.it (W. Cabri), francesco.gasparrini@uniroma1.it (F. Gasparrini).

0021-9673/$ – see front matter © 2011 Elsevier B.V. All rights reserved.
doi:10.1016/j.chroma.2011.04.048

of protein PMTs [16]. The sites of these modifications can be localized by either tandem mass spectrometry of the intact proteins, peptide mass fingerprinting following proteolysis, or a combination of these two techniques. Direct coupling of reversed-phase HPLC with mass spectrometry (HPLC–MS) allowed a comprehensive profiling of core histones and characterization of post-translationally modified isoforms for each histone [16–20].

Despite the dramatic progress in the development of specialized MS technologies for "deciphering the combinatorial histone code" [21], a few efforts have been dedicated to improve selectivity and efficiency of the separation, which are fundamental to address the combinatorial complexity of reversible multi-site modifications of histones. In fact, since 1986 [22], the most widely chromatographic supports explored were C4 [19,23,24] and C18 [25–29] reversed-phase columns, based on porous silica gel microparticles (1.9–5.0 μm) with pore sizes in the 175–300 Å range. Hydrophilic interaction chromatography (HILIC) was successful as well in separating and characterizing different histone isoforms [30,31]. Only recently, the potential of capillary monolithic columns was explored in the isoform separation of a multi-acetylated protein [32] and in combination with free-flow electrophoresis (FFE) for the accurate molecular weight analysis by FT-ICR mass spectrometry [33]. We recently prepared polymethacrylate-based monolithic HPLC columns by means of γ-radiation induced polymerization inside fused-silica capillaries (250–75 μm I.D.) [34]. Such polymerization process has already proved very useful to yield monoliths with various sizes, shapes and porosity features [35–37]. In general, monolithic columns lead to high peak capacity for large biomolecules, and have high through-pore volumes, which provide low back pressure and hence increased mass transfer and flow-rates relative to bead columns. Together, these factors lead to shorter separation times and more efficient separations [38–48]. For these reasons, in this paper we applied our highly efficient monolithic supports in the capillary(nano)-LC/MS profiling of core histone variants and their post-translationally modified isoforms from NCI-H460 human non-small-cell lung cancer (NSCLC) and HCT-116 human colorectal carcinoma cells. The study was extended to monitoring the level of histone acetylation, a very specific covalent PTM, after inhibition of Histone DeACetylase (HDAC) enzymes. Such enzymes represent a new therapeutic target for cancer, since it has been shown that HDACs inhibitors (HDACi) are able to reverse aberrant epigenetic changes associated with cancer [49].

2. Experimental

2.1. Materials

Fused-silica capillary tubings of 250, 200, 100, and 75 μm I.D. and 375 μm O.D. with a polyimide outer coating were purchased from Polymicro Technologies (Phoenix, AZ, USA). HPLC grade solvents for chromatographic separations were from Merck (Darmstadt, Germany). Formic acid (FA), trifluoroacetic acid (TFA), heptafluorobutyric acid (HFBA), hexyl methacrylate (HexMA), ethylene glycol dimethacrylate (EGDMA), 1-propanol, 1,4-butanediol, 2,2-diphenyl-1-picrylhydrazyl hydrate (DPPH). Deionized (18 MΩ) water, purified using a Milli-Q system (Millipore, Milford, MA, USA), was used for preparation of samples and mobile phase solutions. Proteins were quantified using a protein assay kit (Pierce Biotechnology, Rockford, lL, USA). Nitrocellulose membranes were purchased from Bio-rad (Hercules, CA, USA). NuPAGE 4–12% polyacrylamide gel was from Invitrogen (France). Anti-acetyl histone H4 antibody (06-598) and anti-histone H4 antibody (07-108) were from Millipore. NCI-H460 human non-small-cell lung cancer (NSCLC) and HCT-116 human colorectal carcinoma cell lines were purchased from ATCC (Manassas, VA, USA). Suberoylanilide hydroxamic acid (SAHA) was from sigma-tau S.p.A. (Pomezia, Italy).

2.2. Instrumentation and columns

Liquid chromatography was performed using a Micro/Capillary/Nano HPLC system (Model UltiMate 3000, Dionex, Sunnyvale, CA, USA) equipped with two low-pressure gradient micropumps (Model DGP-3600M), a vacuum degasser (Model DG-1210), a micro-autosampler (Model WPS-3000TPL), and a UV-detector (Model VWD-3100, cell 20 nl). The integrated column oven (Model FLM 3100) (5–85 °C temperature range) is provided with a microcolumn switching unit and a flow-splitting device (flow splitter 1:6, 1:100 or 1:1000 for micro-, capillary or nano-analysis, respectively). A linear ion trap mass spectrometer (LXQ, Thermo, San José, CA, USA) equipped with a modified spray capillary TaperTip™, New Objective, 150 μm tubing O.D. and 50 μm tip I.D. standard ESI (>200 μm I.D. capillary columns, connecting tube 30 μm I.D.) or nano ESI (<100 μm I.D. nano-columns, connecting tube 20 μm I.D.) ion source was used for histone identifications. A quadrupolar ion trap mass spectrometer (LCQ Deca, Thermo) equipped with a modified spray capillary TaperTip™, New Objective, 150 μm tubing O.D. and 50 μm tip I.D. standard ESI (>200 μm I.D. columns, connecting tube 30 μm I.D.) was also used only for comparison purposes.

Chromatographic data were collected using the Thermo Xcalibur Chromatography Manager (version 1.2) and the Dionex Chromeleon Datasystem softwares (version 6.80), for MS and UV data processing, respectively. Deconvoluted ESI mass spectra of histones were obtained by using the MagTran 1.02 software. SEM images were acquired with a LEO 1450 VP field emission scanning electron microscope (LEO Electron Microscopy Ltd., Clifton Road, UK). Samples were covered by sputtering with a thin layer of gold. Diffuse Reflectance Infrared Fourier Transform (DRIFT) spectra were recorded on a Jasco 430 FT-IR spectrometer (Jasco Europe, Cremella, Italy) at a resolution of 4 cm^{-1}.

Lab-made organic monolithic (OM) columns (250 mm length) were used with different internal diameters (I.D.): OM_RP_C_6_250 (250 mm × 250 μm, L × I.D.), OM_RP_C_6_200 (250 mm × 200 μm, L × I.D.), OM_RP_C_6_100 (250 mm × 100 μm, L × I.D.), and OM_RP_C_6_75 (250 mm × 75 μm, L × I.D.). Appropriate trap columns were also used: OM_RP_C_6_250 column (50 mm × 250 μm, L × I.D.) or OM_RP_C_6_200 column (50 mm × 200 μm, L × I.D.) for cap-LC separations, and OM_RP_C_6_100 column (50 mm × 100 μm, L × I.D.) for nano-LC separation.

The following commercially available reversed-phase C4 HPLC columns were also used: Jupiter C4, 300 Å, 5 μm particle size (150 mm × 2.1 mm, L × I.D.) by Phenomenex Inc., Torrance, CA, USA; Symmetry C4, 300 Å, 3.5 μm particle size (150 mm × 1.0 mm, L × I.D.), purchased from Waters (Milford, MA, USA); ACE C4, 300 Å, 5 μm particle size (150 μm × 300 μm, L × I.D.) by Advanced Chromatography Technologies, UK. For comparative purposes, the above Jupiter C4 column was emptied and the stationary phase collected and *ad hoc* repacked into a 150 mm × 300 μm I.D. stainless-steel column.

2.3. Preparation and characterization of the organic monolithic columns

After etching the inner wall surface with 1 M NaOH and 0.1 N HCl, fused silica capillaries (250, 200, 100, and 75 μm I.D.) were silanised by reaction with 3-(trimethoxysilyl)propyl acrylate (50%, v/v in toluene), in the presence of 0.05% inhibitor DPPH (2,2-diphenyl-1-picrylhydrazyl hydrate) [34]. A mixture of monomers (0.30 ml) consisting of 55.3 wt% hexyl methacrylate (HexMA) and 44.7 wt% ethylene glycol dimethacrylate (EGDMA) was dissolved

in a ternary porogen solvent (0.70 ml) consisting of 11.1 wt% water, 1-propanol 47.5 wt % and 1,4-butanediol 41.4 wt% [50].

The polymerization mixture was degassed by helium sparging and then introduced into the pre-treated capillary using a slight argon pressure. The ends of the capillary column were finally sealed and the filled capillary was placed inside a Gammacell and irradiated at a temperature of 25 °C with a total dose of 40 KGy, with a dose rate of about 2 KGy/h. After the polymerization was completed, the monolithic column was washed using an HPLC pump with 50 column dead volumes of acetone under constant pressure (10 MPa), to remove unreacted monomers and porogenic solvents.

2.4. Cell culture and treatment with SAHA

The day before the experiment, NCI-H460 human non-small-cell lung cancer (NSCLC) and HCT-116 human colorectal carcinoma cells (2.0×10^6) were seeded in 100 mm × 20 mm dishes, in complete medium (RPMI medium supplemented with 10% v/v foetal bovine serum) and allowed to grow for 24 h before being exposed to SAHA. Cells were then treated for 3 h with SAHA initially dissolved in DMSO and then further diluted in complete medium to reach a final concentration of 0.2% (v/v). Dose-response curves were finally tested. Cells only treated with vehicle (DMSO) were used as control. Following treatments, cells were harvested by scraping by means of a rubber policeman, washed twice with Dulbecco's PBS 1× free of Ca/Mg supplemented with NaB 5 mM 4 °C and resuspended in 200 μl of HNB (0.5 M sucrose, 15 mM Tris/HCl pH 7.5, 60 mM KCl, 0.25 mM EDTA pH 8, 0.125 mM EGTA pH 8, 0.5 mM spermidine, 0.15 mM spermine, 1 mM DTT, 0.5 mM PMSF) and Complete Mini Protease Inhibitor tablets by Roche (Indianapolis, IN, USA). Then, 100 μl of HNB supplemented with 1% NP-40 was added dropwise. After 5 min of incubation at 4 °C, nuclei were pelleted by centrifugation at 2000 × *g* for 3 min with 5 mM NaB. The supernatants could be recovered at this step as cytoplasmatic fraction.

2.5. Histone extraction and Western blot analysis

Histones, acid soluble proteins, were isolated from nuclei by suspension in 0.4 N H_2SO_4 (100 μl), and incubation at 4 °C for 1 h. After centrifugation for 5 min at 10,000 × *g*, histones were precipitated from the supernatant by acetone (1 ml) placed at −20 °C overnight, and then air-dried. The proteins were resuspended in deionized water, quantitated using a Protein assay kit, and then frozen at −80 °C prior to further processing. Notably, freshly prepared solutions are needed to detect H3 histone variants. Purified histones (approximately 4 μg) were loaded onto NuPAGE 4–12% polyacrylamide gel and transferred to a nitrocellulose membrane. Acetylation of histone H4 was detected by Western blot analysis with anti-acetyl histone H4 antibody, and normalized for total histone H4 with anti-histone H4 antibody.

2.6. Cap(nano)-LC/ESI-MS analysis

Cap-LC separations were carried out under reversed-phase conditions on two lab-made organic monolithic OM_RP_C_6_250 (250 mm × 250 μm, L × I.D.) and OM_RP_C_6_200 (250 mm × 200 μm, L × I.D.) capillary columns, thermostated at 60 °C. The flow-rates were 15 μl/min and 10 μl/min, respectively. The mobile phases A and B consisted of 95/5 water/acetonitrile (v/v) (plus 0.05% TFA) and 5/95 water/acetonitrile (v/v) (plus 0.05% TFA), respectively, and were used in linear or segmented gradients, followed by column regeneration and equilibration. The autosampler was thermostated at 5 °C and the samples (0.3–0.4 mg/ml) were injected in partial-loop mode (200 nl). UV detection was performed at 214 nm. Mass spectrometric parameters for histone identifications were as follows: (1) standard ESI, ion polarity, positive; capillary temperature, 400 °C; source voltage, 6.0 kV; capillary voltage, 26 V; tube lens off, 120 V; any sheat or auxiliary gas was used; (2) nano-ESI, ion polarity, positive; source voltage, 2.25 kV; capillary voltage, 4 V; tube lens off, 90 V; any sheat or auxiliary gas was used.

The mass chromatograms were recorded in total ion current (TIC), within 500 and 2000 amu. The signal-to-noise (s/n) ratios of the response were calculated on the unsmoothed mass spectra, with reference to the base peak in the mass spectrum.

Direct injection and load-trapping injection modes for samples were performed (Fig. S1 of Supplementary data) using a 10-port switching valve connected to a loading pump (L.P.), a micropump (μ.P.), a trap column (50 mm length) and a separation column (250 mm length). Both trap and separation column contain the OM_RP_C_6 monolith. In the direct injection mode, the trap column is excluded. In the load-trapping injection mode, sample is introduced onto the loading column (valve in position 10_1) using the L.P. with mobile phase A delivered at 10 μl/min (for OM_RP_C_6_200) and 15 μl (for OM_RP_C_6_250) for 5 min, transferred to the separation column (valve in position 1_2) using the μ.P. with a 2 min linear gradient from 5% to 18% of mobile phase B at 10 μl/min, and finally eluted with a 15 min linear gradient from 18% to 35% of B at 10 μl/min.

2.7. Data processing with ClustMass software

The lab-made ClustMass software employed in the semi-automated analysis of the mass spectrometric detection data was written in Fortran 95 and compiled by the Lahey/Fujitsu Fortran 95 package, LF95 version 5.50. Elaboration of mass data related to HDAC-inhibition by SAHA involving histone H4 was performed by setting the following user-parameters: MR_1 = 11,200; MR_2 = 11,500; TV = 3; MW_1 = 6; PU = 50; MW_2 = 5 (for definitions, see Section 3.4). The fitting procedure on the scatter-graph generated by plotting the *ic* concentrations of SAHA versus the related IE_{ic} values was carried out by Microcal™ Origin software, version 6.0.

3. Results and discussion

3.1. Synthesis of the organic monolithic capillary columns

Capillary columns were prepared by a two-step procedure based on a pre-treatment of the capillary inner walls followed by filling the activated capillaries with the polymerization mixture and irradiation with γ-rays at room temperature. The inner walls of fused-silica capillary were subjected to standard etching protocols to activate the silica surface and then treated with a silane containing methacryloyl fragments in order to ensure immobilization of the growing polymer monolith at the capillary wall [34]. After filling the activated capillary with a degassed solution comprising monomer, cross-linker and a ternary porogen solvent [50], radiation-triggered polymerization was accomplished by exposing the filled capillary to γ-rays at room temperature. A total dose of 40 KGy was sufficient to give a nearly quantitative monomer to polymer conversion, as evidenced by gravimetric analysis of polymer monoliths prepared in larger vessels and by FT-IR spectroscopy.

3.2. Characterization of the organic monolithic capillary and nano-columns

Complete conversion of the monomer and cross-linker mixture to the polymeric monolith was demonstrated by FT-IR spectra of the final material, which showed the disappearance of the absorption bands of the vinyl fragments at 1640 and 3100 cm^{-1}. Scanning

electron microscopy (SEM) of the bulk material and of the monolith prepared inside a fused-silica capillary clearly showed the typical microglobular structure of organic monoliths (Fig. S2 of Supplementary data), together with micrometer-sized open channels that are essential to assure a free flow to the liquid phase at low pressure. Close inspection of SEM pictures taken on the whole capillary showed a uniform filling of the inner space within the column and firm contacts of the monolith with the column walls, indicating an effective polymerization process and a covalent attachment of the polymer to the inner surface of the walls. This, in turn, resulted in a mechanically stable monolith that resists extrusion from the column, and that has no void spaces in proximity of the walls because polymer shrinkage during polymerization was minimized.

Flow resistance properties of the monolithic columns were ascertained by monitoring the pressure drop across 250 mm length columns at varying flow-rates using a water–acetonitrile 40/60 (v/v) mobile phase. Strictly linear plots were obtained for a linear velocity range extending from 0.20 to 11.0 mm/s, indicating complete absence of compression phenomena of the monolith in response to pressure stress. For the OM_RP_C_6_250 column, the column permeability K_0 and the specific permeability K_F were calculated according to Eqs. (1) and (2), where μ_0 represents the linear flow velocity, η is the viscosity of the solvent, L is the column length, Φ is the flow-rate, r is the radius of column and ΔP_c is the pressure drop across the column.

$$K_0 = \frac{\mu 0 \eta L}{\Delta P_c} \quad (1)$$

$$K_F = \frac{\eta L \phi}{r^2 \pi \Delta P_c} \quad (2)$$

$$K_F = K_0 \times \varepsilon_T \quad (3)$$

With a mobile phase consisting of water/acetonitrile 40/60 (v/v), and using a value for its viscosity $\eta = 0.72 \times 10^{-3}$ Pa s at 25 °C, Eqs. (1) and (2) gave permeability values $K_0 = 5.81 \times 10^{-14}$ m^2 and $K_F = 4.07 \times 10^{-14}$ m^2, with a total porosity $\varepsilon_T = 0.70$ (calculated by Eq. (3)). The good permeability obtained allowed the use of high eluent flow-rates under "high speed" conditions, and could in principle be used for the preparation of longer columns affording increased resolution and peak capacity.

Chromatographic behavior of the prepared monoliths was tested using a protein mixture sample containing lysozyme, α-lactalbumin, β-lactoglobulin and carbonic anhydrase, spanning a molecular mass range from 14 to 29 kDa. The separations were carried out using either the direct injection or the load-trapping mode approaches (see Fig. S1 of Supplementary data), with the latter featuring a short (50 mm length) OM_RP_C_6 column as trapping device (200 or 250 μm I.D.). A detailed description of proteins separation is provided in Supplementary data (Table S1 and Figs. S3–S4).

3.3. Cap(nano)-LC/ESI-MS method development

The main purpose of the present study was to develop a reliable and efficient capillary and nano-LC/ESI-MS method for the fast separation of histone variants and their post-translationally modified isoforms. In fact, each histone peak comprised a population of molecules that can differ in the type and number of PTMs. Such sequence variants often differ by only a few amino acids [9,20]. Coupling of HPLC to a mass spectrometer allows for the determination of the masses of the constituent isoforms. In order to accomplish this task, we performed baseline separation of six unfractionated acid-extracted histone proteins (namely, H2A-1, H2A-2, H2B, H4, H3-1, and H3-2) on lab-made monolithic columns, prepared by γ-radiation induced polymerization inside fused-silica capillaries. The analytical method, based on reversed-phase conditions with ion pairing additives, was improved by optimization of ion pairing agent and temperature, such that sequence variants were readily resolved. Moreover, once found the best chromatographic conditions, the LC/MS method was scaled-down from capillary to nano-scale columns (*i.e.,* from 250 μm internal diameter to 200, 100, and 75 μm); gradient slope and flow-rate were optimized accordingly. Injection of samples was obtained by the use of a micro-autosampler, both in the direct and load-trapping injection modes.

3.3.1. Effect of the ion pairing agent

Separation of highly basic proteins by RP-HPLC normally requires the use of ion pairing agents such as trifluoroacetic acid (TFA) and heptafluorobutyric acid (HFBA), due to their high content in basic amino acid residues (*e.g.,* lysine and arginine). Such additives are typically used to increase analyte hydrophobicity by forming ion pairs with the charged groups, and to enable protein defolding as well, which makes accessible their buried hydrophobic groups [51]. Although the use of ion paring agents is necessary, it yields adducts that complicate the mass spectra and decrease the limit of detection [20,29]. Therefore, ESI-MS detection sensitivity must be checked, with different ion-paring agents, before developing a suitable HPLC–MS method.

At this purpose, we compared the effect of formic acid (FA), heptafluorobutyric acid (HFBA) and trifluoroacetic acid (TFA) as ion pairing additives for the cap(nano)-LC/ESI-MS separation of six intact core histones (H2A-1, H2A-2, H2B, H4, H3-1 H3-2), with the aim of improving detection sensitivity (*i.e.,* ionization intensity of histone proteins) while achieving baseline resolution and a suitable selectivity between the different variant peaks.

FA at a concentration of 0.4% (v/v) in water/acetonitrile mobile phases yielded poor peak shape and the lowest selectivity, in particular, for histones H2B and H4 which were co-eluted (see Fig. 1a). Moreover, histone H3-1 was eluted in the tail of H2A-2. The separation obtained with HFBA (0.04%) was also unsatisfactory (data not shown), since significant signal suppression was observed and poor selectivity performances were reached. TFA is a typical signal suppressor in ESI-MS, since it forms very strong ion pairs with analytes that are not efficiently broken in the ESI interface, thus lowering ionization. Despite such drawback, however, TFA is an excellent ion-pairing agent for the separation of proteins by RP-HPLC, usually used at 0.1% concentration. For this reason, we used TFA at a lower concentration (0.05%) and obtained excellent performances in terms of selectivity, resolution and peak shape (see Fig. 1b), allowing the complete separation of the six histones. Furthermore, at this low TFA amount, the decrease in MS sensitivity could be regained by the increased analyte concentrations due to sharpened peaks. Further improvement of the MS sensitivity was observed upon down-scaling the column internal diameter to 75 μm and transferring to the nano-ESI interface (see Fig. 1c): a signal-to-noise ratio equal to 154 was recorded for the mass spectrum collected on histone H2A-1 peak.

3.3.2. Effect of column temperature

High-temperature liquid chromatography proved useful in the separation of intact proteins [52]. Increasing the column temperature, in fact, may modify the column surface properties and alter protein structure, thus affecting their retention. Moreover, analyte sorption kinetics increases with temperature, minimizing band broadening and improving column efficiency [52]. However, most conventional packed reversed-phase columns experience few problems at temperatures higher than 50 °C, preventing their use under such temperature conditions for prolonged times. On the contrary, monolithic columns do not get a waiver from the consequences of these heat effects [38], and higher temperatures may be used for very long times. We evaluated the effect of column temperature on histone separation by raising the OM_RP_C_6_200

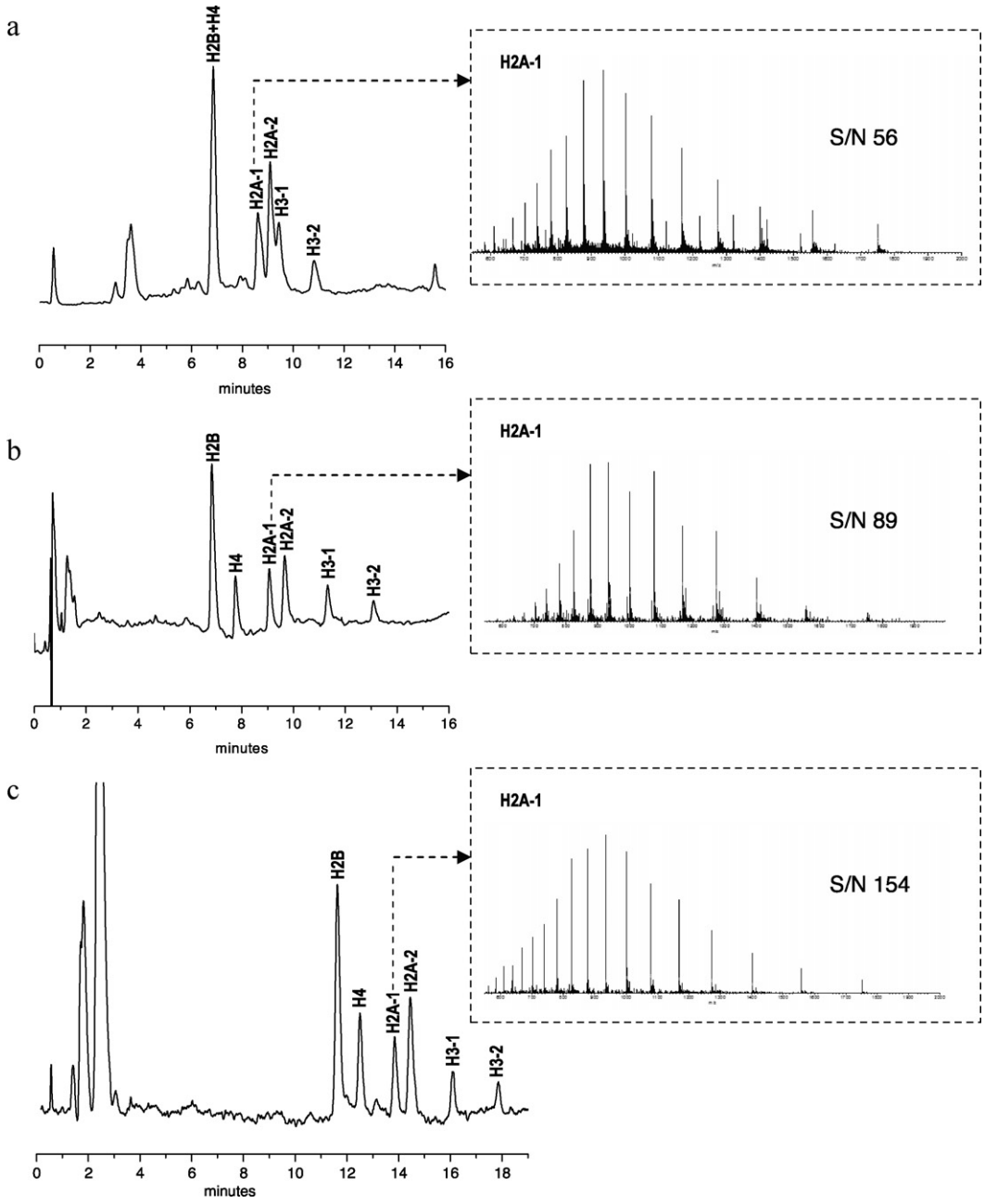

Fig. 1. Effect of ion pairing agent in the separation of intact histones from NCI-H460 human non-small-cell lung cancer (NSCLC) cell lines. Direct injection mode. (a) Column: OM_RP_C_6_200 (250 mm × 200 μm, L × I.D.). Mobile phases, A = water/acetonitrile 95/5 (v/v) + 0.4% FA; B = water/acetonitrile 5/95 (v/v) + 0.4% FA. Flow-rate: 13 μl/min. Detection: standard ESI-MS, total ion current (TIC) from 500 to 2000 amu; ion polarity, positive; capillary temperature, 400 °C; source voltage, 6.0 kV; capillary voltage, 26 V; tube lens off, 120 V. Linear gradient from 18% to 35% of B for 16 min, followed by column regeneration and equilibration for 4 min. T = 60 °C. (b) Column: OM_RP_C_6_200 (250 mm × 200 μm, L × I.D.). Mobile phases, A = water/acetonitrile 95/5 (v/v) + 0.05% TFA; B = water/acetonitrile 5/95 (v/v) + 0.05% TFA. Flow-rate: 13 μl/min. Detection: standard ESI-MS (see above). (c) Column: OM_RP_C_6_75 (250 mm × 75 μm, L × I.D.). Mobile phases, A = water/acetonitrile 95/5 (v/v) + 0.05% TFA; B = water/acetonitrile 5/95 (v/v) + 0.05% TFA. Flow-rate: 1.8 μl/min. Detection: nano-ESI-MS; source voltage, 2.25 kV; capillary voltage, 4 V; tube lens off, 90 V; any sheat or auxiliary gas was used. Insets: mass spectra collected on histone H2A-1 peak.

column temperature from 25 to 60 °C. At room temperature and flow-rate of 6.0 μl/min, separation of the six histone variants was unsatisfactory (Fig. 2a). By increasing the temperature to 40 → 60 °C (Fig. 2b–d), mobile phase viscosity and back pressure were reduced, allowing the use of higher flow-rates which had a favourable impact on run times. In particular, flow-rate was increased to 10 μl/min (μ_0 = 7.58 mm/s) and three temperatures (40, 50, and 60 °C) were compared. The best results were obtained at 60 °C, where the high temperature improved resolution and efficiency, but also yielded strong histone ionization. Notably, an inversion of the elution order for H2A-1 and H4 peak was observed, by heating the column from 25 °C to 40 → 60 °C, as judged by the relative retention time (RRT) values to H2B peak calculated (Fig. 2).

Long-term use of the OM_RP_C_6 supports showed relatively high performances in terms of retention factors and selectivity after 1000 injections for the direct injection mode, and 2000 injections for the load-trapping mode.

3.3.3. Comparison with packed columns

Chromatographic separation of intact proteins has been traditionally accomplished using packed columns with alkylated silica based stationary phases. Some problems associated with

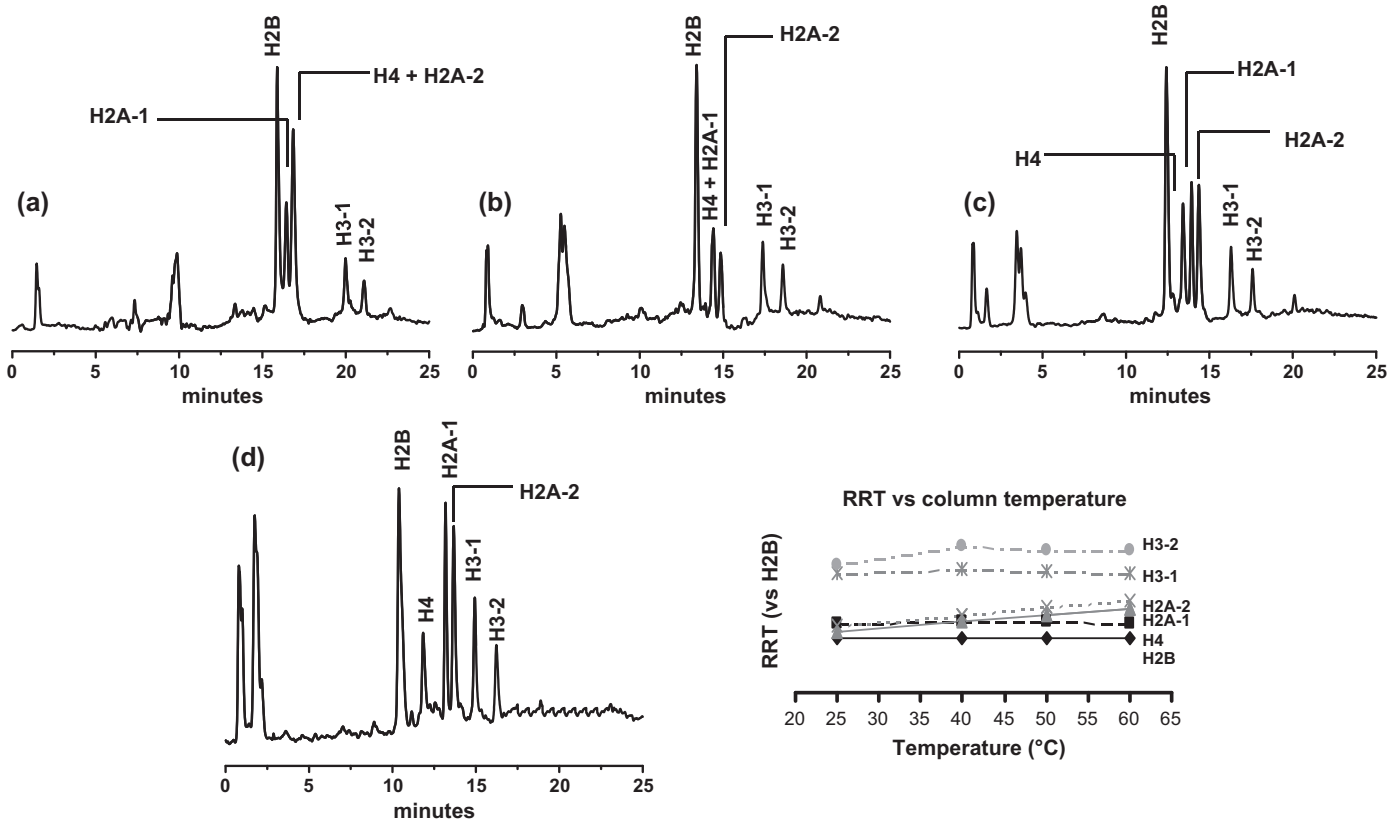

Fig. 2. Effect of column temperature in the separation of intact histones from NCI-H460 cell lines. Column: OM_RP_C_6_200 (250 mm × 200 μm, L × I.D.). Mobile phases, A = water/acetonitrile 95/5 (v/v) + 0.05% TFA; B = water/acetonitrile 5/95 (v/v) + 0.05% TFA. Linear gradient from 18% to 25% of B in 10 min; to 40% B in 10 min; at 40% B for 10 min, followed by column regeneration and equilibration for 4 min. Detection: UV at 214 nm. (a) T = 25 °C and flow-rate: 6.0 μl/min. (b) T = 40 °C and flow-rate: 10 μl/min. (c) T = 50 °C and flow-rate: 10 μl/min; (d) T = 60 °C and flow-rate: 10 μl/min.

this approach are related to the chemical nature of the stationary phase that may generate irreversible adsorption on unreacted and exposed silanols and poor peak shapes, due to slow desorption from the silica surface. Additionally, severe back pressure limitations are encountered when small particle size and high eluent flow-rates are used in concert for high-throughput applications. In an attempt to compare the overall performances of our monolithic columns with conventional packed columns, we investigated the separation capabilities of an ACE C4, 300 Å, 5 μm particle size (150 μm × 300 μm, L × I.D.) capillary column and of a lab-packed capillary column containing the Jupiter C4 300 Å, 5 μm stationary phase (150 mm × 300 μm, L × I.D.). Since the capillary version of the Jupiter C4 column was not commercially available, the stationary phase was collected from a 150 mm × 2.1 mm, L × I.D. column and *ad hoc* repacked into a 150 mm × 300 μm L × I.D. stainless-steel column. Efficiency tests towards a set of small molecules were performed on the column before starting the investigation on histones. A Symmetry C4, 300 Å, 3.5 μm particle size (150 mm × 1.0 mm, L × I.D.) column was also included in the comparative study. The intact histone mixture from NCI-H460 cell lines was separated on the packed capillary columns using two gradient elution profiles, with total gradient times of 30 min, for the ACE C4 column (Fig. 3a) and 60 min, for the Jupiter C4 one (Fig. 3b). The six histone components gave clearly resolved peaks on both columns, although with partial overlapping of the H4 and H2A-1 components. Using a linear flow velocity (μ_0) of 0.78 mm/s, the total analysis time was around 30 min on the ACE C4 column and 45 min on the Jupiter C4 one. Separation of the histone mixture could also be obtained on the OM_RP_C_6_200 monolith column, under similar experimental conditions, using again two gradient elution profiles, with total gradient times of 5 and 15 min (Fig. 3c and d, respectively). The much faster gradients could be used here because of the optimal selectivity showed by the polymethacrylate-based stationary phase. Notably, our OM_RP_C_6_200 column showed superior selectivity compared to packed C18 Ultra High Performance Liquid Chromatography (UHPLC) [29] or polystyrene-divinylbenzene monolithic [32,33] columns for the core histones H2A, H2B, H3 and H4, that are usually eluted within narrow time windows and are therefore poorly resolved. Given the larger permeability of the OM_RP_C_6_200 monolithic column, linear flow velocities up to ~11 mm/s could be used, leading, in the case of the fast gradient, to a total analysis time of 8 min (Fig. 3c). Elution at μ_0 = 7.58 mm/s with the 15 min gradient time led to a total analysis time of 15 min and to an increased resolution, as evidenced by the splitted peaks observed for the linker H1 histone variants (Fig. 3d).

Chromatographic profiles of intact histones obtained on the Symmetry C4 300 Å, 3.5 μm column are shown in Supplementary data (Fig. S5). Elution at a linear flow velocity of 1.17 mm/s led to an increased resolution among the six histone peaks, but with a total analysis time of 80 min.

3.3.4. Scaling-down and flow-rate optimization

Analytical separations using HPLC with small-diameter columns have recently become an indispensable tool in protein characterization, where sample volume and concentration are often limited. The reduction of column internal diameter from 250 to 75 μm was performed at lower and higher linear flow velocity (Fig. 4); we investigated the effect of flow-rate and gradient slope on both chromatographic performances and detection sensitivity (Fig. S6 of Supplementary data). Detailed results are presented in Table 1.

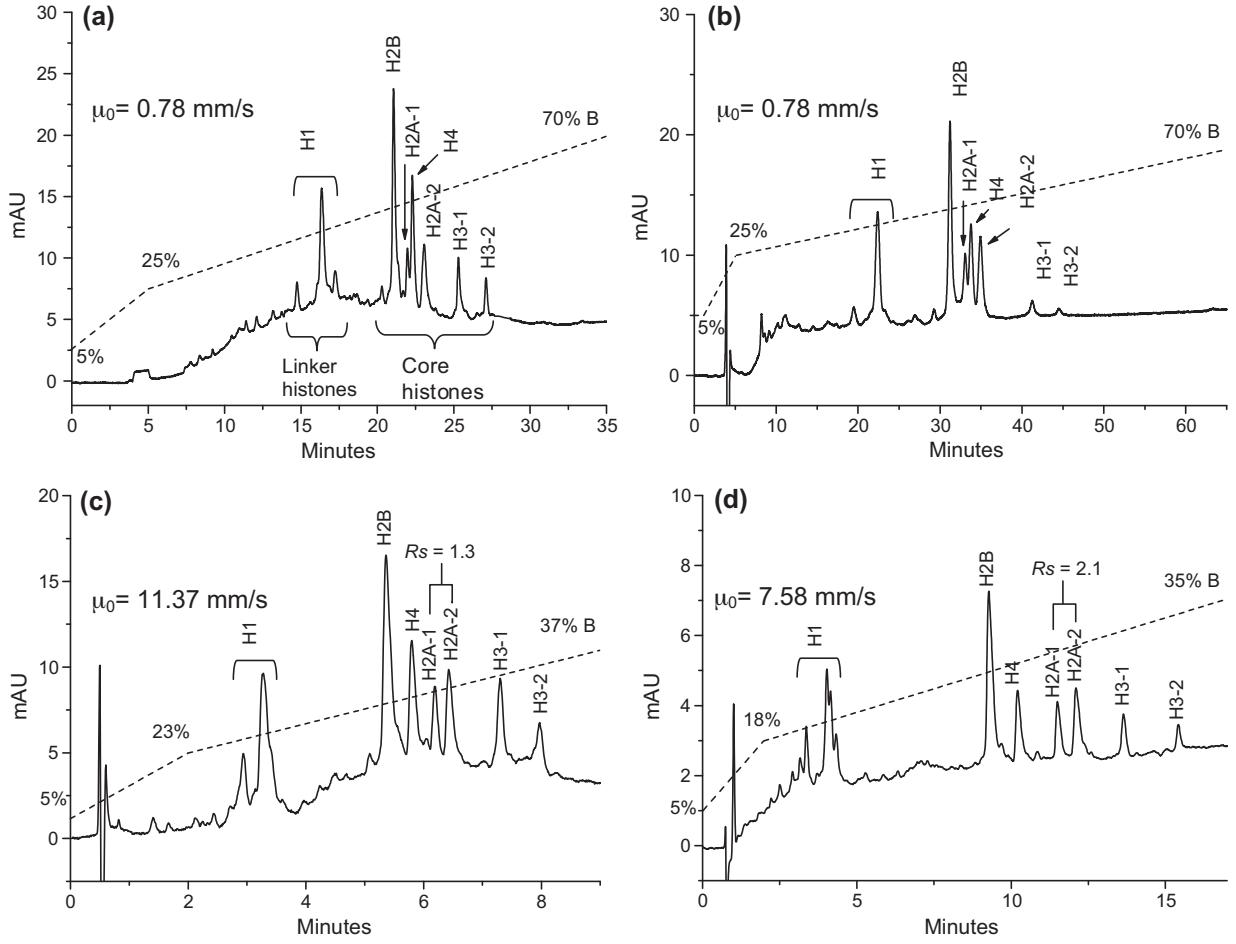

Fig. 3. Comparison of (a) the packed capillary ACE C4 300 Å, 5 μm (150 mm × 300 μm, L × I.D.) column and (b) the repacked Jupiter C4 300 Å, 5 μm (150 mm × 300 μm, L × I.D.) column with the monolithic OM_RP_C_6_200 (250 mm × 200 μm, L × I.D.) column (c,d) in the separation of intact histones from NCI-H460 cell lines. Mobile phases, A = water/acetonitrile 95/5 (v/v) + 0.1% TFA; B = water/acetonitrile 5/95 (v/v) + 0.1% TFA. Linear gradient from 5% to 25% of B in 5 min; to 70% of B in 30 min (a) and in 60 min (b) at a flow-rate of 3.0 μl/min (μ_0 = 0.78 mm/s), at T = 25 °C. Linear gradient from 5% to 23% of B in 2 min; to 37% of B in 5 min (c) at a flow-rate of 15 μl/min (μ_0 = 11.37 mm/s), at T = 60 °C. Linear gradient from 5% to 18% of B in 2 min; to 35% of B in 15 min (d) at a flow-rate of 10 μl/min (μ_0 = 7.58 mm/s), at T = 60 °C. Detection: UV at 214 nm, cell volume: 20 nl. Injected volumes: 500 nl (a and b) and 200 nl (c and d).

Table 1
Effect of flow-rate reduction on both chromatographic performances and detection sensitivity for the separation of six intact histones from NCI-H460 human non-small-cell lung cancer cell lines. For chromatographic conditions, see Fig. 4 (*higher linear velocity*).

Column	OM_RP_C_6_250		OM_RP_C_6_200		OM_RP_C_6_100		OM_RP_C_6_75	
Internal diameter (μm)	250		200		100		75	
Flow-rate (μl/min)	20		13		3.2		1.8	
μ_0 (mm/s)	9.70		9.85		9.70		9.70	
Δpi (bar)	200		210		240		230	
Gradient time (min)	15		15		18		20	
Injected volume (nl)	200		~150		~30		~20	
Injected amount (ng)	70		~50		~10		~7	
S/N (by MS)[a]	100		125		150		250	
Chromatographic parameters	PWHH (s)	*Rs*	PWHH (s)	*Rs*	PWHH (s)	*Rs*	PWHH (s)	*Rs*
H2B	6.6		9.6		10.8		10.8	
		2.83		3.44		3.33		2.96
H4	7.2		9.0		9.6		10.2	
		5.04		5.03		4.47		4.65
H2A-1	9.0		9.6		10.8		10.2	
		2.09		2.09		1.95		1.89
H2A-2	10.2		10.8		12.0		12.0	
		6.03		5.69		5.86		5.38
H3-1	9.0		9.6		8.4		10.2	
		6.72		6.37		7.45		6.34
H3-2	8.4		9.6		7.8		9.6	
Mean	8.4	4.54	9.7	4.52	9.9	4.61	10.5	4.24

[a] Standard-ESI-MS (for capillary OM_RP_C_6_250–200 μm I.D. columns); nano-ESI-MS (for nano OM_RP_C_6_100–75 μm I.D. columns).

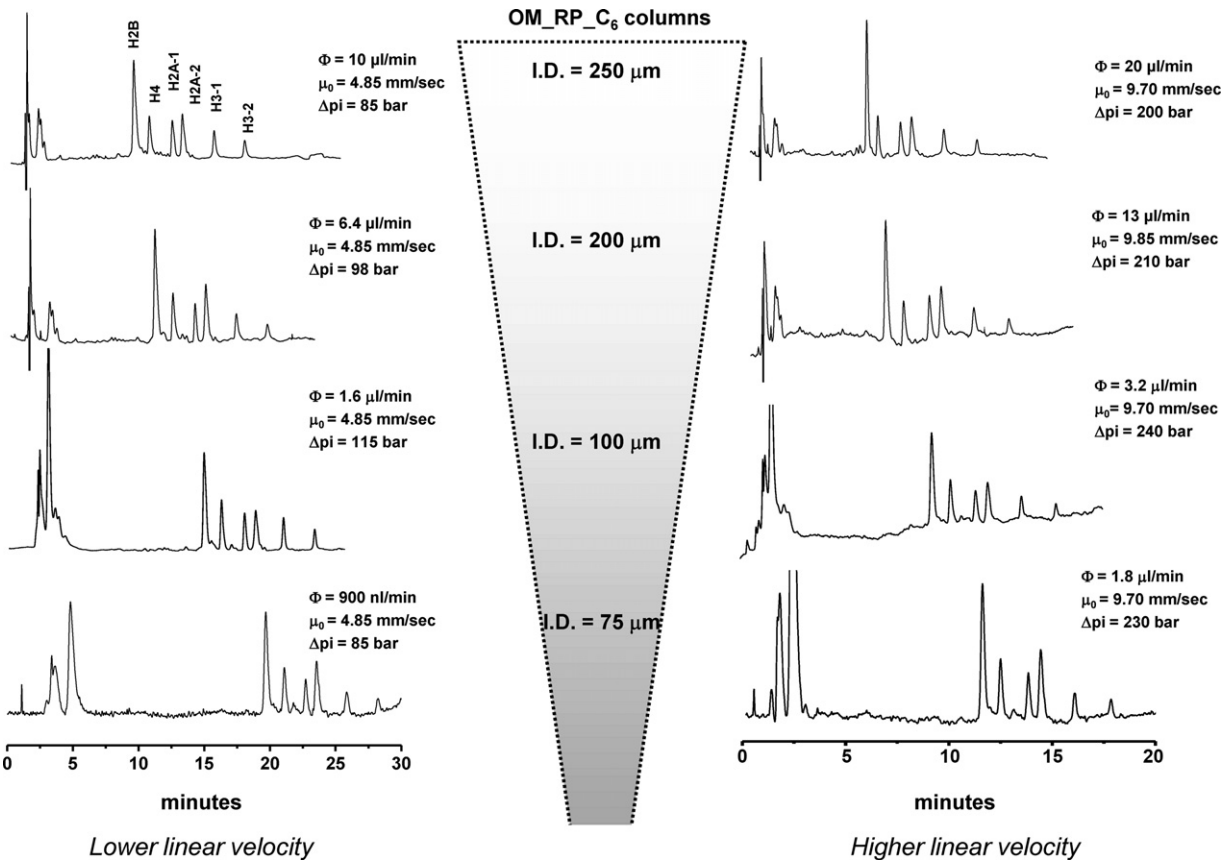

Fig. 4. Scaling-down of histones chromatographic separation. Reduction of OM_RP_C_6 columns I.D. from 250 to 75 μm was performed at lower and higher linear velocity. Mobile phases, A = water/acetonitrile 95/5 (v/v) + 0.05% TFA; B = water/acetonitrile 5/95 (v/v) + 0.05% TFA. Linear gradient from 18% to 35% of B (see Table 1 for gradient times), followed by column regeneration and equilibration for 4 min. T = 60 °C. Detection: standard ESI-MS (for OM_RP_C_6_250–200 columns) and nano-ESI-MS for OM_RP_C_6_100–75 columns).

The high permeability of our monolithic materials enables the use of flow-rates even 10-fold higher than those attainable with packed columns, thus allowing rapid separation with comparable back pressure and reduced time analysis. At high linear velocity, the gradient slope has further been optimized taking into account the effect of void volumes (Figs. S7 and S8 of Supplementary data). Resolution factor (R_S) obtained for each couple of histone peaks demonstrates the baseline resolution at each column diameter with an average PWHH from 8.4 to 10.5 s (see Table 1).

Moreover, as expected, the column miniaturization has resulted in higher protein concentrations within smaller peak volumes, thus enabling more sensitive MS detection; in fact, for a concentration-sensitive device, the detector signal depends on the concentration of the analyte in the carrier flow. In particular, for histone detection, we obtained an average signal-to-noise (s/n) ratio of the mass spectra larger then 100 upon further downscaling from capillary to nano-HPLC (Table 1 and Fig. 1c).

In order to establish whether the standard ESI interface could compromise peak shape due to ion suppression or enhancement, we compared PWHHs obtained by UV and MS detection for the same chromatographic run on the OM_RP_C_6_250 analytical column. Similar average PWHHs values were observed (10.1 s for UV and 11.8 for MS), demonstrating that any peak broadening is caused by the ESI interface (Fig. S9 of Supplementary data and Table 1).

Higher values of PWHH achieved for histone peaks with respect to values obtained for protein test mixture (see Section 3.2) can be attributed to a partial separation of the post-translational isoforms. As shown in Fig. S10 of Supplementary data, analysis of mass spectra collected at selected retention time windows within a single peak, showed that peak broadening is due to the diverse level of hydrophobicity of PTMs (methylation, acetylation, etc.) occurring within a single histone variant.

3.4. ClustMass software development

The analysis of peptides and proteins is facilitated by the generation of multiply charged species. Multiple charging makes it possible to analyze a broad range of molecular weights by collecting data over a narrow range of mass-to-charge (m/z) ratios. However, multiple charging complicates interpretation of a spectrum because the charge state of an ion must be determined before the molecular weight can be assigned. Programs to perform deconvolution process are generally included as part of the data system software for instruments capable of collecting ESI data. Unfortunately, most require some interaction with the user in order to correct for artefacts created by the deconvolution process and insure proper charge state assignment. Moreover, analysis of the hundreds of spectra generated by a single HPLC/MS run is very tedious and prone to human error.

We developed a computer program that we called ClustMass aimed at rapidly and semi-automatically processing all the spectra in an LC/MS run by the use of a relevant algorithm. The final goal was to elaborate and evaluate experimental data in a format that can be easily visualized, and to quantify the ability of a given molecular species $\boldsymbol{I_n}$ to inhibit HDAC enzymes, *i.e.,* to evaluate its capability to behave as HDAC inhibitor (HDACi). For this purpose, we defined a proper Relative half maximal Inhibitory Concentration (IC_{50}) parameter, that we called R_IC_{50}.

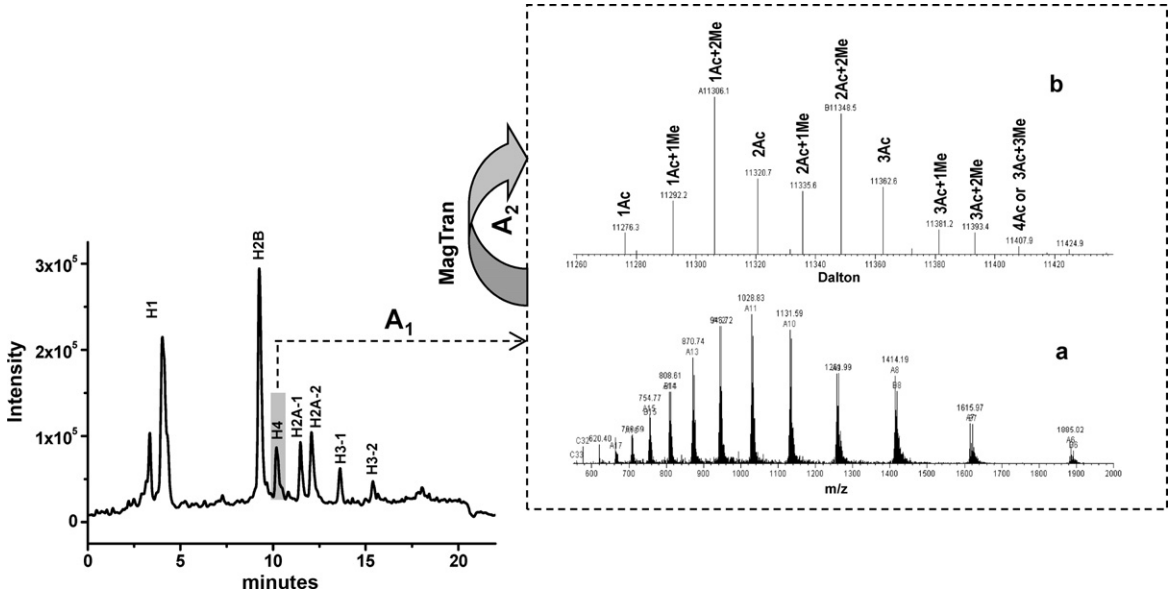

Fig. 5. Mass spectrum extraction (subsection A1) and deconvolution by MagTran 1.02 software (subsection A2) for histone H4 peak. Insets: (a) ESI-MS full-scan spectrum recorded from 600 to 2000 amu. (b) Corresponding deconvoluted spectrum with relative peaks assignment. Chromatographic conditions are as described in Fig. 3d.

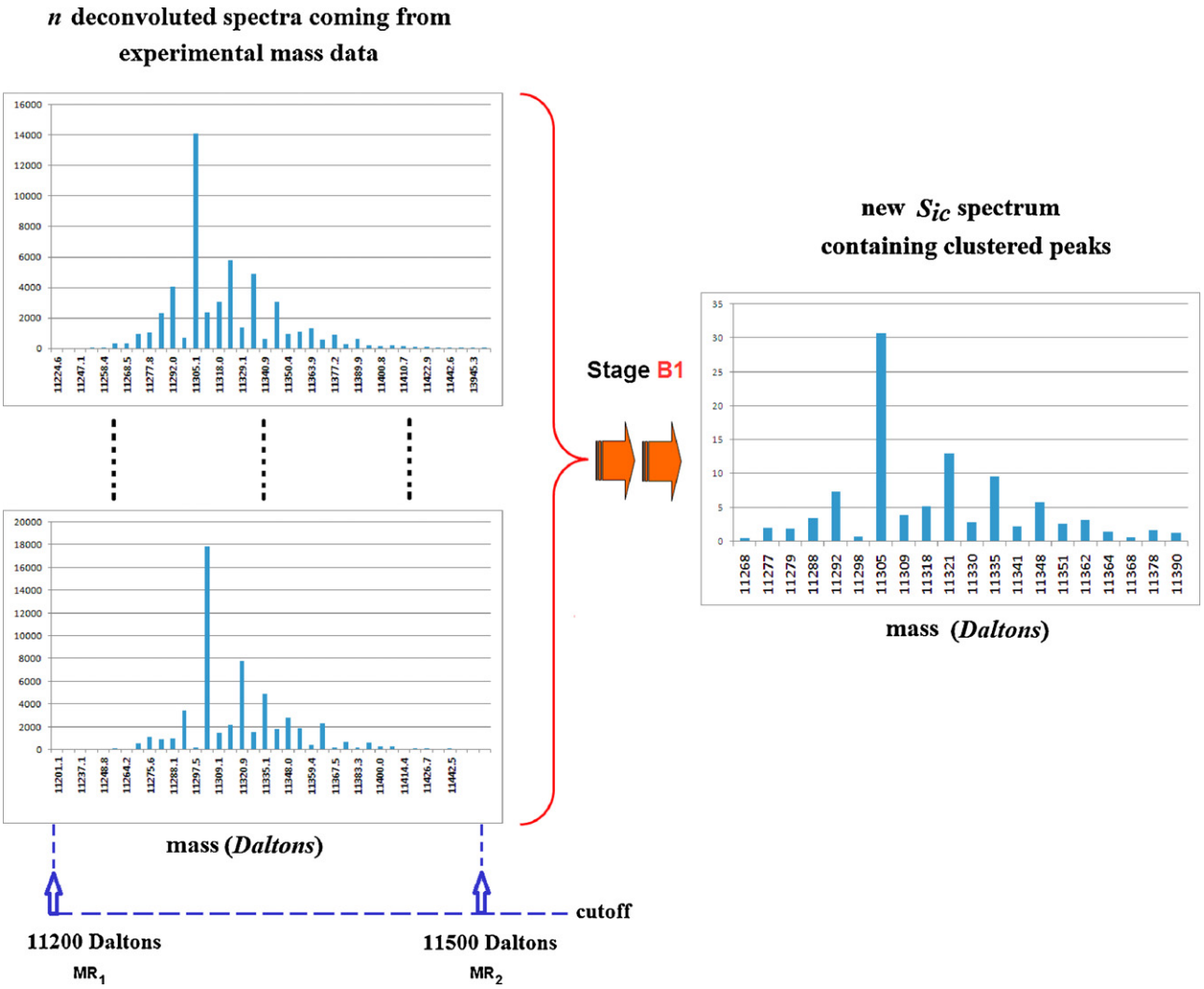

Fig. 6. Automated clusterization of peaks contained into experimental deconvoluted mass spectra (at least two replicates) and their insertion into a new representative S_{ic} spectrum by ClustMass program (stage B1 of the algorithm).

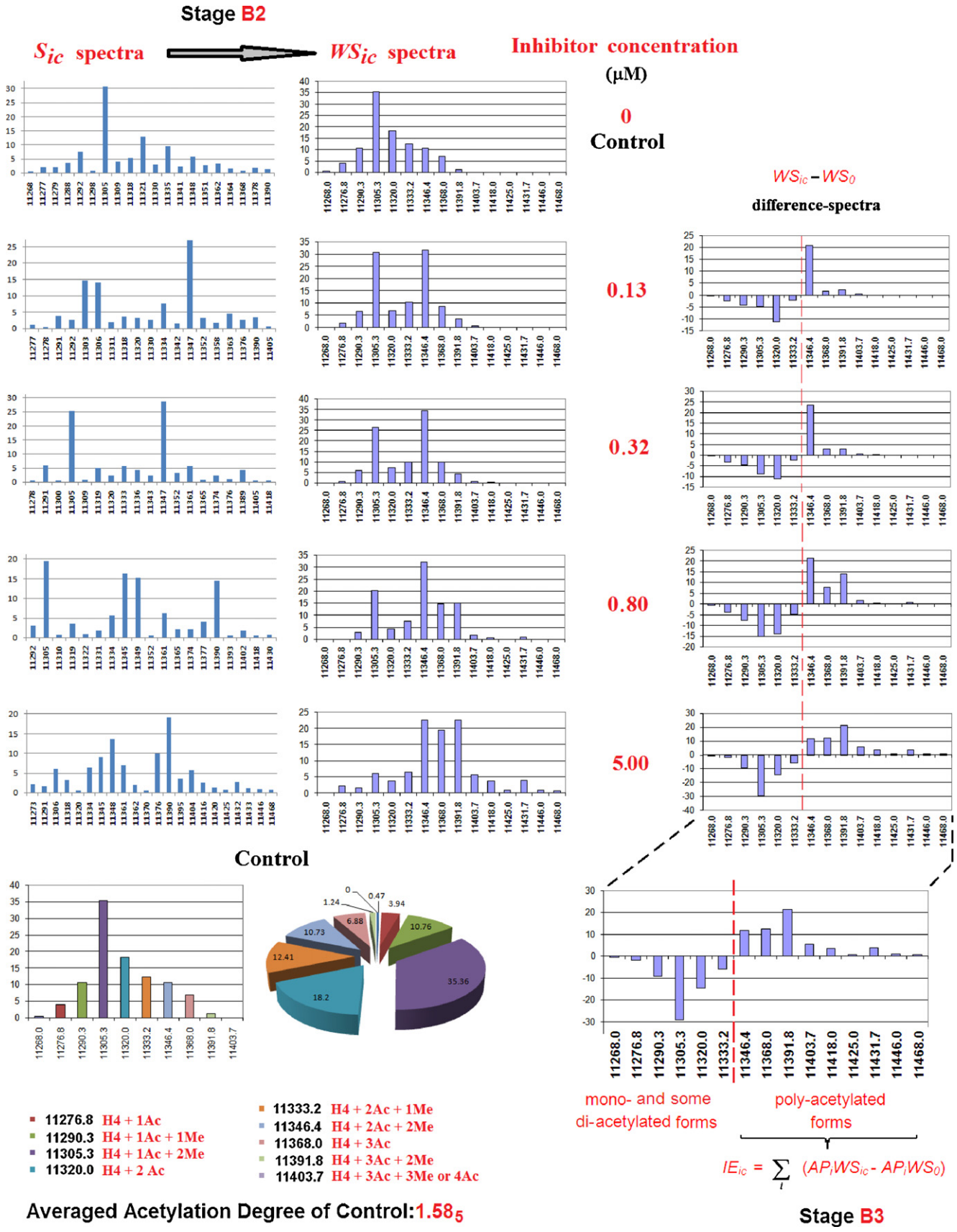

Fig. 7. ClustMass elaboration of S_{ic} spectra to new mass-aligned WS_{ic} spectra (stage B2 of the algorithm) and comparison between WS_{ic} spectra obtained at different HDACi concentrations (0.13–5.00 μM) and control WS_0: calculation of the IE_{ic} factor (stage B3 of the algorithm).

The whole procedure was organized into two principal sections run in duplicate, A (manual) and B (automated by ClustMass), and is described using a generic experimental set-up in which an HDACi (namely, SAHA) is used at five different concentrations (including a control experiment at zero concentration) and its effects are observed on the six different core histones extracted from NCI-H460 cancer cells.

Section A is composed by two A1 and A2 subsections (see Fig. 5): in the first one (A1), the raw multi-charged mass spectra (m/z) manually extracted from a TIC for a given chromatographic peak are collected from two replicate runs, and these two m/z mass spectra are manually uploaded to and elaborated by MagTran 1.02 deconvolution software, yielding two deconvoluted mass spectra (Dalton) for each of the six chromatographic peaks for each of the five inhibitor concentration, totalling 60 deconvoluted mass spectra (subsection A2).

In section B, the deconvoluted mass spectral data are uploaded to ClustMass to be automatically elaborated into three algorithm stages, B1, B2, and B3, in seconds time-scale. In stage B1, mass spectral data are treated to round the masses to the nearest integer and exclude peaks either outside a chosen range of masses (MR_1, MR_2) or endowed with intensities below a threshold value (TV). MR_1, MR_2 and TV are all parameters defined by the user, the first two specifically dependent from the mass of the analyzed histone, the third one typically set as equal or less than 3% of the most abundant peak. Then, from the ensemble of the so elaborated spectra, for each core histone at each inhibitor concentration, *ic*, it is obtained a new spectrum (S_{ic}, Fig. 6) containing clustered peaks, normalized to provide 100% as the sum of all peak abundances, resulting from the averaged masses of peaks within an imposed mass-window (MW_1), and endowed with abundances different not more than an imposed amount of percentage units (PU). Thus, MW_1 and AP are two further user-defined parameters, the first one typically set to 5–6 Da, the second to a value not far from 50%.

In the next stage of the algorithm (B2), with the intent to allow a direct comparison, all the S_{ic} spectra (30 coming from stage B1) are further treated to ensure the same rank of mass values (*i.e.,* the same values of *x*-coordinate) to each of them. Such new elaborated ensembles of mass spectral data will be hereafter symbolized as WS_{ic}. The goal is achieved by merging one to each other the peaks considered as belonging to a common and narrow window of masses (a new user-defined parameter, MW_2, typically set to 5 Da), and assigning to each of such new clustered peaks a mass value averaged from those proper of the parent peaks. As it may be easily seen by inspection of Fig. 7, at a progressive decrease of abundance of the peaks related to the mono- and some di-acetylated forms of histone H4 (peaks <11,350 Da) corresponds an equivalent overall growth of abundance of peaks related to the poly-acetylated forms.

Finally, in the last stage of the algorithm (B3), each WS_{ic} spectrum (30 for stage B2) relative to an inhibitor concentration different from zero is compared to the control (that is, the spectrum WS_0 relative to zero concentration of inhibitor). Thus, the extent of inhibition (IE_{ic}) at each *ic* concentration of $\boldsymbol{I_n}$ is evaluated by summing the differences of the same sign calculated between the Abundances of Peaks of equal mass (AP_iWS_{ic}) across the spectra WS_{ic} (with $ic \neq 0$) and WS_0:

$$IE_{ic} = \sum_i (AP_iWS_{ic} - AP_iWS_0)$$

(sum extended to only positive differences) (4)

This amount expresses in a cumulative way all changes underwent by the primary structure of histone as a result of the HDAC-inhibition by $\boldsymbol{I_n}$, when compared to control. Figure 7 refers to the case of histone H4 and shows the increasing of HDAC inhibition, expressed by IE_{ic} values, as a function of increasing of the $\boldsymbol{I_n}$ concentration, *ic*. The trend of such a scatter-plot may be conveniently fitted by non-linear analysis by Eq. (5):

$$IE_{ic} = \left(-\exp\left(\frac{-ic}{\mathrm{P1}}\right) + 1\right) \times \mathrm{P2} \quad (5)$$

The P1 and P2 parameters, achievable by the aforementioned regression analysis, afford decisive information about the studied inhibition process. Indeed, coefficient P2 expresses the maximum extent of HDAC-inhibition (IE_{max}) that, relatively to the control, $\boldsymbol{I_n}$ can show when it is added in concentration numerically much greater than the value assumed by P1. In other words, P2 represents the IE_{ic} value corresponding to the plateau reached by Eq. (5) at properly high concentrations of $\boldsymbol{I_n}$. Instead, P1 affords a practical way to calculate R_IC_{50}, which represents the I_n concentration responsible for an HDAC inhibition level amounting to 50% of IE_{max} (*i.e.,* to P2/2). In fact, R_IC_{50} can be calculated by resolving Eq. (5) with respect to the independent variable *ic* and imposing IE_{ic} equal to $IE_{max}/2$ (*i.e.,* P2/2):

$$\frac{IE_{max}}{2} = \left(-\exp\left(\frac{-R\_IC_{50}}{\mathrm{P1}}\right) + 1\right) \times \mathrm{P2} \quad (6)$$

After suitable rearrangement, Eq. (6) affords the final expression for the evaluation of

$$R\_IC_{50} : R\_IC_{50} = \mathrm{P1} \times \ln(2) \quad (7)$$

Regression analysis (see Fig. 8) afforded a R_IC_{50} value of 0.27 μM for SAHA with regard to NCI-H460 cell lines. By applying the same approach to HCT-116 cells, we obtained for SAHA a R_IC_{50} value of 0.23 μM (see also Section 3.5).

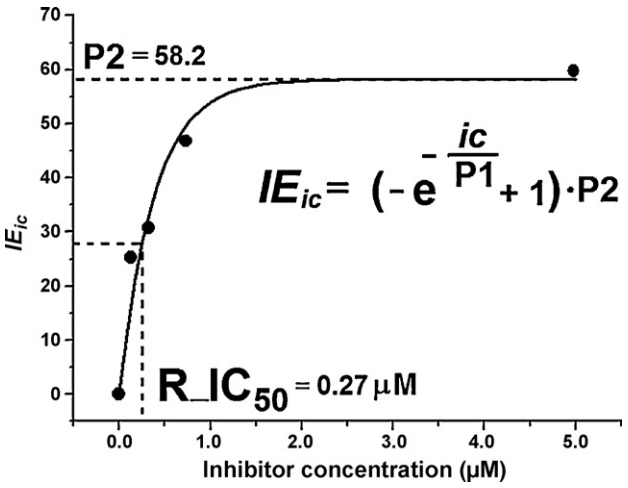

Fig. 8. Calculation of R_IC_{50} of SAHA for NCI-H460 cell lines by ClustMass software.

3.5. Evaluation of HDAC inhibitors

Although the mapping and characterization of histone PTMs have progressed rapidly in the past decade, importance or function of each individual modification is still far from being understood [16]. To increase our depth of understanding in this field it is helpful to obtain also quantitative information.

The cap-LC/MS method here described provide a rapid and reliable tool to obtain a global view of all six core histones and their PTMs. Changes in modification levels for each histone can be monitored at each inhibitor concentration. Moreover, quantitative parameters such as R_IC_{50} and averaged acetylation degree can be

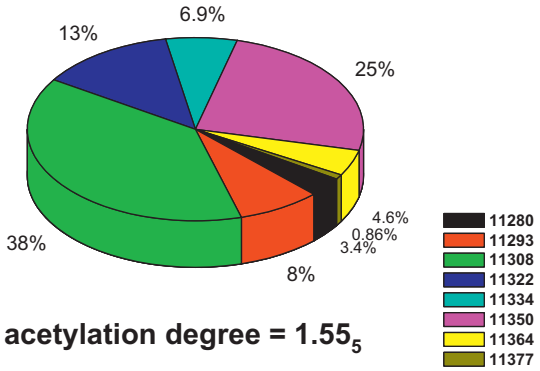

Fig. 9. Post-translational modifications distribution and calculation of average acetylation degree for histone H4 from control HCT-116 cells (*i.e.*, cells only treated with vehicle (DMSO), see Section 2.4).

calculated for each histone to compare different HDACi by evaluating their inhibitory potency, or to investigate their selectivity towards HDAC of different classes.

Experiments were carried out on two different cancer cell lines that exhibit different global HDAC activity as well as different response to HDACi. In particular, NCI-H460 and HCT-116 cells were treated with increasing concentrations of SAHA (0–5 μM for NCI-H460 and 0–7 μM for HCT-116) and, as expected, results showed that all core histones displayed hyperacetylation profiles with the administration of increased level of SAHA. In particular, for each inhibitor concentration and for each histone, the PTMs pattern was obtained by using the ClustMass software, as described in Section 3.4. Fig. 9 shows the results, in a graphical form, of a control experiment at zero inhibitor concentration for histone H4 from HCT-116 cell lines, which gave an averaged acetylation degree of 1.55$_5$. Acetylation degree was calculated according to Eq. (8).

$$\text{Acetylation degree} = \frac{\sum_{\text{max\_}nAc}^{\text{max\_}nAc} \text{max\_}nAc \times \sum_i AP_i^{nAc} WS_{ic}}{100} \quad (8)$$

where the first summation extends from the mono-acetylated (*nAc* = 1) to the poly-acetylated form, with *max_nAc* equal to the maximum number of acetyl fragments found in a given histone, and the second summation considers the peak abundances AP_i of the *i*th peak with the same number of acetyl groups *nAc* in a given final spectrum WS_{ic} at a given inhibitor concentration *ic*. The three-dimensional bar plot in Fig. 10 compares the control experiment (blue bars) with two experiments performed with added SAHA inhibitor at 0.4 and 0.8 μM concentrations (red and green bars, respectively). The isobaric acetylation and trimethylation were indistinguishable at the current mass resolving power and chromatographic resolution. Thus it is impossible to unambiguously assign a unique isoform to each peak in the deconvoluted spectrum. The overall effect of incremental addition of SAHA is visually evident from the shift of the elaborated spectral peaks towards high-mass values, corresponding to an increase of the averaged acetylation degree from 1.55$_5$ (no inhibitor added) to 2.65 (0.4 μM SAHA added) and 4.07 (0.8 μM SAHA added), corresponding to an R_IC$_{50}$ value of 0.23 μM (see also Section 3.4). When PTMs of the other histones H2B, H2A-2, H3-1 and H3-2 were followed using the same scatter plots (Fig. 11), we observed similar pattern modifications with high-mass range shifts that were more pronounced at higher SAHA concentrations.

The obtained R_IC$_{50}$ values were in agree with those achieved by Western-blot analysis using anti-acetyl histone H4 and anti-histone H4 antibodies (IC$_{50}$ = 0.48 μM for NCI-H460 cell lines). However, it is to take into consideration that, despite being highly sensitive, immunoassay methods are just qualitative and furthermore they can give false readings from neighbouring modifications affecting antibody binding.

The overall procedure for the evaluation of HDACi by cap(nano)-LC coupled with MS and combined with the ClustMass software routine proved fast and highly sensitive at the same time, as evidenced from daily throughput data collected in Table 2. With 250 mm long columns, a single LC–MS run is completed within 25 and 30 min, when working in direct injection or load-trapping mode (including re-equilibration and automatic injection time) approach, respectively. These short analysis times could be easily obtained thank to the combination of the high selectivity and permeability of the monolithic columns. In particular, the high permeability allowed us to use flow-rates of 15 and 1.5 μl/min on the capillary (250 μm I.D.) and nano (75 μm I.D.) columns, respectively: accordingly, the daily throughput was 58 and 48 samples in the direct injection and load-trapping mode approach, respectively. The overall throughput could be improved by a factor of 2–3 when working in the *high speed mode* (see Fig. 3c), which allows to reach 8 min time windows and linear eluent velocities up to 11 mm/s.

Sample consumption is also a key factor to consider when a complete screening of PTMs is planned for several potential HDACi. Using samples with total histone concentrations in the 0.3–0.4 mg/ml range, a single run required about 70 ng of histones injected on the capillary column (250 μm I.D.), and only 6.5 ng to be injected on the nano-column (75 μm I.D., see Table 2).

Table 2
Daily throughput data of the cap- and nano-LC organic monolithic columns.

	Cap-LC (OM_RP_C$_6$_250)		Nano-LC (OM_RP_C$_6$_75)	
	Direct injection	Load-trapping[a]	Direct injection	Load-trapping[a]
Flow-rate	15 μl/min	15 μl/min	1.5 μl/min	1.5 μl/min
Run time	25 min	25 + 5 min	25 min	25 + 5 min
Mobile phase volume[b]	375 μl	450 μl	37.5 μl	45 μl
Sample injected amount[c]	~70 ng		~6.5 ng	
Daily required sample amount	4.06 μg	3.36 μg	0.377 μg	0.312 μg
Daily required mobile phase	21.6 ml		2.16 ml	
Daily throughput	58	48	58	48

[a] Trapping time: 5 min; trap column geometry: 50 mm × 250 μm, L × I.D. for cap-LC and 100 μm for nano-LC.
[b] Total volume of mobile phase used for each run time analysis (run time × flow-rate).
[c] Sample protein concentration: 0.3–0.4 mg/ml; for injected volumes, see Table 1.

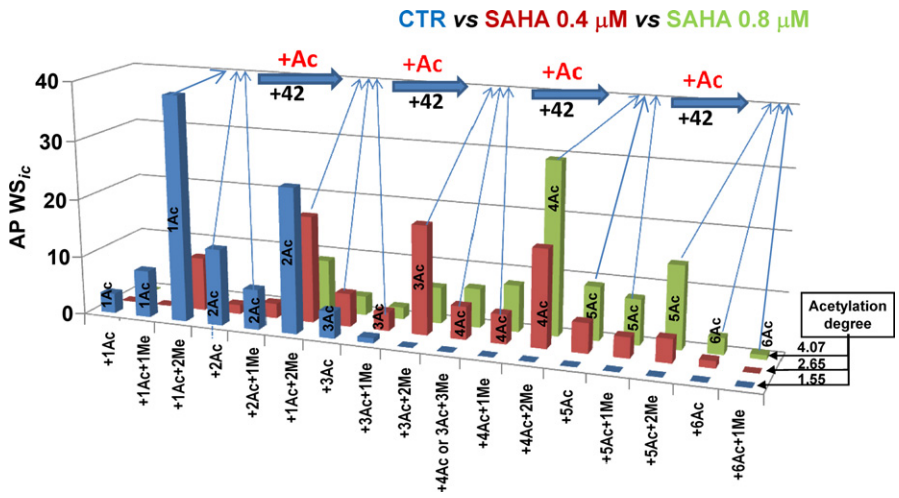

Fig. 10. Three-dimensional bar plots showing all post-translational modifications for core histone H4 from control HCT-116 cells (CTR, blue bars, *ic* = 0), cells treated with 0.4 μM SAHA (red bars, *ic* = 0.4), and 0.8 μM SAHA (green bars, *ic* = 0.8). (For interpretation of the references to color in this figure legend, the reader is referred to the web version of the article.)

These features are superior in terms of speed of analysis and sample consumption when compared with similar LC–MS methods based on microbore columns (2.0 μm I.D.) packed with C4, 5 μm silica particles [19], where total analysis time of 60 min was reported to accomplish a complete resolution of the histone components in samples with 1 mg/ml protein concentrations (10 μg injected).

Analysis time and sample consumption of our chromatographic method are also reduced compared to a UHPLC approach based on narrow-bore columns packed with 1.9 μm C18 silica particles [29], where total run time of 19 min and sample loading of 10 μg of acid-extracted histones were reported. When the fast histone separations reported on packed HPLC [19] and UHPLC [29] columns are compared with the high speed separations of the present work (see Fig. 3c), it appears that our monolithic columns can withstand much larger linear eluent velocities (11.37 mm/s versus 0.53 and 1.44 mm/s of the HPLC and UHPLC columns, respectively), without a significant loss of efficiency.

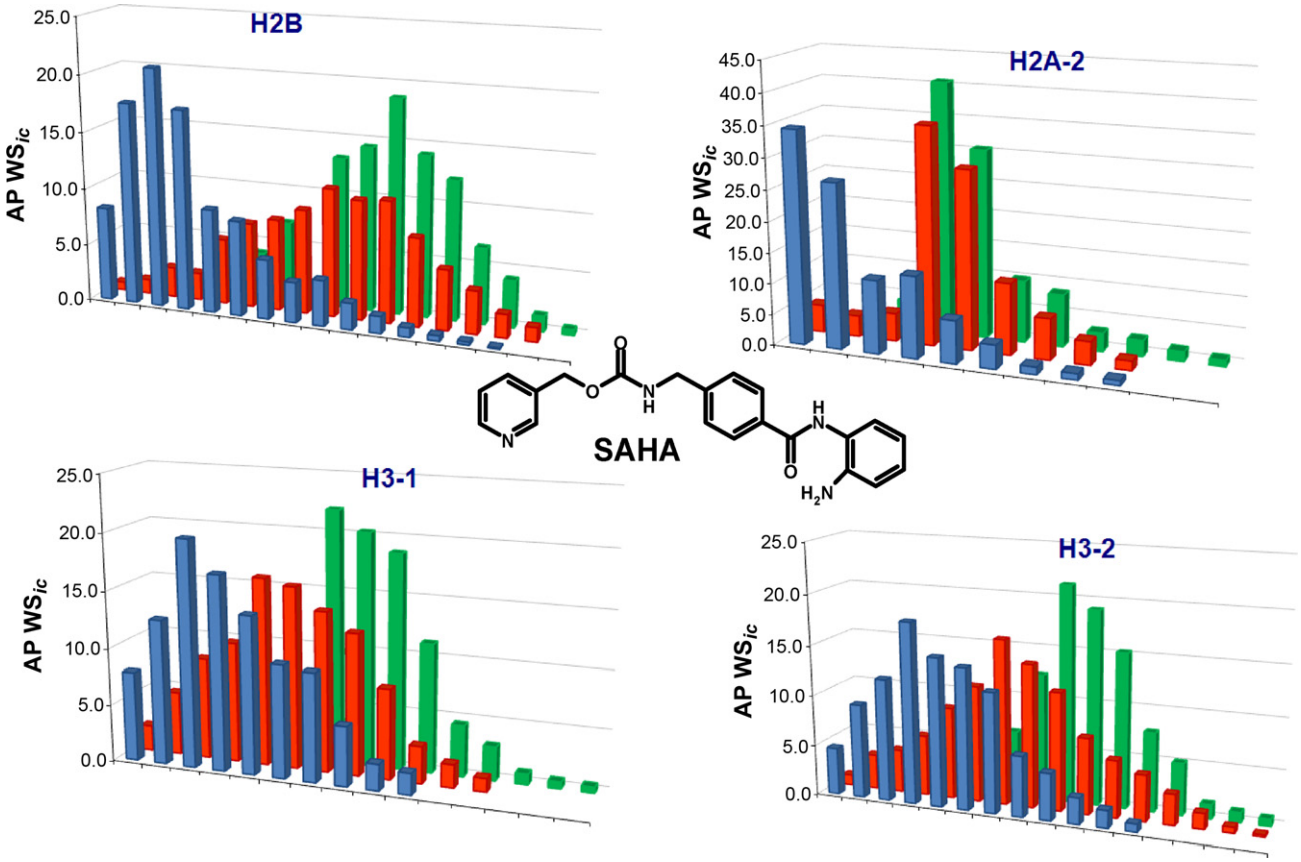

Fig. 11. Comparison of post-translational modifications for core histones H2A-2, H2B, H3-1, and H3-2 from control HCT-116 cells (blue bars, *ic* = 0), cells treated with 0.4 μM SAHA (red bars, *ic* = 0.4), and with 7.0 μM SAHA (green bars, *ic* = 7.0). (For interpretation of the references to color in this figure legend, the reader is referred to the web version of the article.)

4. Conclusions

Monolithic HPLC columns with capillary and nano formats were prepared by γ-radiation induced polymerization of methacrylate monomers and cross-linkers in the presence of porogenic solvents. The overall performance of the columns, evaluated using four standard proteins, was excellent in terms of efficiency, stability, and permeability and allowed fast separations under gradient elution conditions. The monolithic columns were the core of an HPLC–MS method for the evaluation of histones post-translational modifications and, in combination with the lab-made software routine ClustMass, for the study of histone acetylation after inhibition of HDAC enzymes by SAHA.

Compared to existing methods for the HPLC analysis of intact histones and of their PTMs, the newly developed method based on lab-made monolithic columns offers shorter analysis times combined with large selectivity, efficiency and reduced sample requirements. Indeed, the development of fast and precise technology based on the use of small amount of biological samples is driving the drug discovery process. Moreover, the understanding of the biological modifications at molecular level is the basis of a modern approach to bioassay. The cap(nano)-LC/MS method that we developed offers the capability to combine LC miniaturization with a fast elaboration process of mass spectral data, which have the fascinating effect to shed light on the study of histone PTMs. In particular, ClustMass proved to be a versatile tool in elaborating deconvoluted mass spectral data (aligning, averaging, clustering), which could be potentially employed to discriminate the degree of histone acetylation.

Acknowledgements

We are grateful for financial supports from FIRB, Research program: Ricerca e Sviluppo del Farmaco (CHEM-PROFARMA-NET), grant no. RBPR05NWWC_003, and from Sapienza Università di Roma, Italy (Fund for selected research topics 2009, grant no. C26A094JH2). We thank Dr. Zhongqi Zhang (Amgen Inc., Thousand Oaks, CA, USA) for providing MagTran 1.02 software.

Appendix A. Supplementary data

Supplementary data associated with this article can be found, in the online version, at doi:10.1016/j.chroma.2011.04.048.

References

[1] T. Jenuwein, C.D. Allis, Science 293 (2001) 1074.
[2] G. Felsenfeld, M. Groudine, Nature 421 (2003) 448.
[3] K. Sandman, S.L. Pereira, J.N. Reeve, Cell. Mol. Life Sci. 54 (1998) 1350.
[4] C.A. Ouzounis, N.C. Kyrpides, J. Mol. Evol. 42 (1996) 234.
[5] A.T. Annunziato, J.C. Hansen, Gene Expr. 9 (2000) 37.
[6] S.L. Berger, Curr. Opin. Genet. Dev. 12 (2002) 142.
[7] T. Kouzarides, Curr. Opin. Genet. Dev. 12 (2002) 198.
[8] J.C. Rice, C.D. Allis, Curr. Opin. Cell Biol. 13 (2001) 263.
[9] S.C. Galasinski, D.F. Louie, K.K. Gloor, K.A. Resing, N.G. Ahn, J. Biol. Chem. 277 (2002) 2579.
[10] K. Zhang, K.E. Williams, L. Huang, P. Yau, J.S. Siino, E.M. Bradbury, P.R. Jones, M.J. Minch, A.L. Burlingame, Mol. Cell. Proteomics 1 (2002) 500.
[11] W. Fischle, Y.M. Wang, C.D. Allis, Curr. Opin. Cell Biol. 15 (2003) 172.
[12] B. Strahl, C.D. Allis, Nature 403 (2000) 41.
[13] B.M. Turner, Cell 111 (2002) 285.
[14] C. Crane-Robinson, T.R. Hebbes, A.L. Clayton, A.W. Thorne, Methods 12 (1997) 48.
[15] N. Suka, Y. Suka, A.A. Carmen, J. Wu, M. Grunstein, Mol. Cells 8 (2001) 473.
[16] B.M. Ueberheide, S. Mollah, Int. J. Mass Spectrom. 259 (2007) 46 (and references cited therein).
[17] K. Zhang, H. Tang, J. Chromatogr. B 783 (2003) 173.
[18] M.A. Freitas, A.R. Sklenar, M.R. Parthun, J. Cell. Biochem. 92 (2004) 691.
[19] M. Naldi, V. Andrisano, J. Fiori, N. Calonghi, E. Pagnotta, C. Parolin, G. Pieraccini, L. Masotti, J. Chromatogr. A 1129 (2006) 73.
[20] X. Su, N.K. Jacob, R. Amunugama, D.M. Lucas, A.R. Knapp, C. Rena, M.E. Davis, G. Marcucci, M.R. Parthun, J.C. Byrd, R. Fishel, M.A. Freitas, J. Chromatogr. B 850 (2007) 440.
[21] J.M. Gilmore, M.P. Washburn, Nat. Methods 4 (2007) 480.
[22] H. Lindner, W. Helliger, B. Puschendorf, J. Chromatogr. A 357 (1986) 301.
[23] S. Olmo, R. Gotti, M. Naldi, V. Andrisano, N. Calonghi, C. Parolin, L. Casotti, V. Cavrini, Anal. Bioanal. Chem. 390 (2008) 1881.
[24] M. Naldi, N. Calonghi, L. Masotti, C. Parolin, S. Valente, A. Mai, V. Andrisano, Proteomics 9 (2009) 5437.
[25] J.Y. Kim, K.W. Kim, H.J. Kwon, D.W. Lee, J.S. Yoo, Anal. Chem. 74 (2002) 5443.
[26] L. Zhang, M.A. Freitas, J. Wickham, M.R. Parthun, M.I. Klisovic, G. Marcucci, J.C. Byrd, J. Am. Soc. Mass Spectrom. 15 (2004) 77.
[27] R.A. Parise, J.L. Holleran, J.H. Beumer, S. Ramalingam, M.J. Egorin, J. Chromatogr. B 840 (2006) 108.
[28] D. Bonenfant, M. Coulot, H. Towbin, P. Schindler, J. van Oostrum, Mol. Cell. Proteomics 5 (2006) 541.
[29] K. Contrepois, E. Ezan, C. Mann, F. Fenaille, J. Proteome Res. 9 (2010) 5501.
[30] H. Lindner, B. Sarg, C. Meraner, W. Helliger, J. Chromatogr. A 743 (1996) 137.
[31] B.J. Garcia, J.J. Pesavento, C.A. Mizzen, N.L. Kelleher, Nat. Methods 4 (2007) 487.
[32] E.-J. Sneekes, M. Damen, R. Swart, A.J.R. Heck, J. Chromatogr. A 1194 (2008) 199.
[33] E.-J. Sneekes, J. Han, M. Elliot, J. Ausio, R. Swart, A.J.R. Heck, C. Borchers, J. Sep. Sci. 32 (2009) 2691.
[34] G. Angelini, O. Ursini, F. Gasparrini, C. Villani, PCT Int. Appl. (2008), WO 2008081496 A1 20080710.
[35] A. Sáfrány, B. Beiler, K. László, F. Svec, Polymer 46 (2005) 2862.
[36] B. Beiler, A. Vincze, F. Svec, A. Sáfrány, Polymer 48 (2007) 3033.
[37] F. Svec, J. Chromatogr. A 1217 (2010) 902.
[38] G. Guiochon, J. Chromatogr. A 1168 (2007) 101.
[39] H. Oberacher, A. Premstaller, C.G. Huber, J. Chromatogr. A 1030 (2004) 201.
[40] L. Trojer, S.H. Lubbad, C.P. Bisjak, G.K. Bonn, J. Chromatogr. A 1117 (2006) 56.
[41] P. Hemström, A. Nordbotg, K. Irgum, F. Svec, J.M.J. Fréchet, J. Sep. Sci. 29 (2006) 25.
[42] L. Trojer, S.H. Lubbad, C.P. Bisjak, W. Wieder, G.K. Bonn, J. Chromatogr. A 1146 (2007) 216.
[43] J. Urban, P. Jandera, J. Sep. Sci. 31 (2008) 2521.
[44] X. Chen, H.D. Tolley, M.L. Lee, J. Sep. Sci. 32 (2009) 2565.
[45] I. Nischang, F. Svec, J.M.J. Fréchet, J. Chromatogr. A 1216 (2009) 2355.
[46] E.G. Vlakh, T.B. Tennikova, J. Chromatogr. A 1216 (2009) 2637.
[47] Y. Li, H.D. Tolley, M.L. Lee, J. Chromatogr. A 1217 (2010) 4934.
[48] S. Eeltink, S. Dolman, F. Detobel, R. Swart, M. Ursem, P. Schoenmakers, J. Chromatogr. A 1217 (2010) 6610.
[49] P.A. Marks, W.-S. Xu, J. Cell. Biochem. 107 (2009) 691.
[50] E.C. Peters, M. Petro, F. Svec, J.M.J. Fréchet, Anal. Chem. 70 (1998) 2288.
[51] T. Greibrokk, T. Andersen, J. Chromatogr. A 1000 (2003) 743.
[52] H. Schlüter, in: M. Kastner, Protein Liquid Chromatography, J. Chromatogr. Lib., vol. 61, Elsevier, Amsterdam, 2000, p. 147.